

# Loschmidt echo and Lyapunov exponent in a quantum disordered system

Y. Adamov,<sup>1</sup> I. V. Gornyi,<sup>2,1,\*</sup> and A. D. Mirlin<sup>1,2,†</sup>

<sup>1</sup>*Institut für Nanotechnologie, Forschungszentrum Karlsruhe, 76021 Karlsruhe, Germany*

<sup>2</sup>*Institut für Theorie der Kondensierten Materie, Universität Karlsruhe, 76128 Karlsruhe, Germany*

(Received 3 December 2002; published 27 May 2003)

We investigate the sensitivity of a disordered system with diffractive scatterers to a weak external perturbation. Specifically, we calculate the fidelity  $M(t)$  (also called the Loschmidt echo) characterizing a return probability after a propagation for a time  $t$  followed by a backward propagation governed by a slightly perturbed Hamiltonian. For short-range scatterers, we perform a diagrammatic calculation showing that the fidelity decays first exponentially according to the golden rule, and then follows a power law governed by the diffusive dynamics. For long-range disorder (when the diffractive scattering is of small-angle character), an intermediate regime emerges where the diagrammatics is not applicable. Using the path-integral technique, we derive a kinetic equation and show that  $M(t)$  decays exponentially with a rate governed by the classical Lyapunov exponent.

DOI: 10.1103/PhysRevE.67.056217

PACS number(s): 05.45.Mt, 03.65.Sq, 73.23.-b, 05.60.Gg

## I. INTRODUCTION

Quantum manifestations of the classical chaotic dynamics represent a central issue for the field of quantum chaos. To characterize quantitatively the stability of quantum motion, Peres [1,2] proposed to consider the fidelity

$$M(t) = |\langle \psi | \exp(i\hat{H}'t) \exp(-i\hat{H}t) | \psi \rangle|^2, \quad (1)$$

where  $\hat{H}'$  differs by a small perturbation from the Hamiltonian  $\hat{H}$  of the system under consideration and  $|\psi\rangle$  is some original state (wave packet). The quantity (1) is the probability to return into the state  $|\psi\rangle$  after propagation for a time  $t$  governed by the Hamiltonian  $\hat{H}$  followed by a backward propagation with a slightly perturbed Hamiltonian  $\hat{H}'$ . Recently, Jalabert and Pastawski [3] argued that for a system whose classical counterpart is chaotic the fidelity (1) will decay exponentially with time, with the rate given by the classical Lyapunov exponent. Their work was motivated by measurements of a spin-echo decoherence rate in nuclear magnetic resonance experiments [4], and they gave a name “quantum Loschmidt echo” to the overlap (1). The paper [3] triggered a considerable outbreak of research activity devoted to the sensitivity of quantum chaotic systems to external perturbations. In a number of subsequent publications [5–18], the Loschmidt echo was studied (predominantly by means of numerical simulations) for a variety of classically chaotic systems and its relation to decoherence problems was discussed. These numerical works have confirmed the key prediction of Ref. [3] that in an appropriate parameter range the decay rate of the Loschmidt echo is governed by the classical Lyapunov exponent.

In the present paper, we study the Loschmidt echo (1) in a different context, namely, that of a *quantum-disordered* system. Specifically, we consider a particle moving in a weak *quantum* random potential. The word “quantum” means here that the scattering on this disorder is of diffractive nature. For a Gaussian random potential assumed here, this is equivalent to the condition

$$d \ll l_s, \quad (2)$$

where  $d$  is the disorder correlation length and  $l_s$  is the quantum mean free path. This situation should be contrasted with the opposite case of a classical disorder, for which the disorder-induced contribution to the action on a distance  $\sim d$  is much larger than  $\hbar$ , and the representation of propagators in terms of a sum over classical orbits (as used, e.g., in Ref. [3]) is justified. On the other hand, the standard theoretical tool for the quantum-disorder regime is the impurity diagram technique. It is therefore natural to attempt to apply the diagrammatics to the Loschmidt echo problem.

We show that indeed the diagrammatic technique can be used to calculate the fidelity for short times (where it is given simply by the golden-rule formula), as well as for sufficiently long times (where it decays according to a power law reflecting the diffusive character of the classical motion). We demonstrate, however, that for a sufficiently smooth [but still quantum as defined by Eq. (2)] disorder an intermediate time range emerges, where the diagrammatic method breaks down. Using the path-integral approach, we calculate the Loschmidt echo in this regime and find that it does show the decay governed by the classical Lyapunov exponent, which is highly nontrivial in view of the diffractive character of disorder.

The rest of the paper is organized as follows. In Sec. II, we consider the case of a short-range disorder ( $d \ll \lambda_0$ , where  $\lambda_0$  is the electron wavelength) when the diagrammatic calculation works in the whole range of times. We identify diagrams corresponding to the short-time (golden-rule) and the long-time (diffusion-induced power law) behavior of the fidelity and evaluate them. Section III, which is the central one

\*Also at A.F. Ioffe Physical-Technical Institute, 194021 St. Petersburg, Russia.

†Also at Petersburg Nuclear Physics Institute, 188350 St. Petersburg, Russia.

for the paper, is devoted to the case of a long-range random potential ( $d \gg \lambda_0$ ) when the scattering is of small-angle character. Our conclusions are summarized in Sec. IV. In particular, we discuss there a connection between the Loschmidt echo problem and a recent activity [19–23] devoted to quantum interference effects in the regime of quantum chaos.

## II. LOSCHMIDT ECHO FOR THE SHORT-RANGE POTENTIAL

As discussed in Sec. I, we consider a model of the particle moving in a random potential inducing a quantum (diffractive) scattering. We will assume the limit of an infinite system size. The Hamiltonians  $H$  and  $H'$  describing the forward and the backward propagation in Eq. (1) correspond to two slightly different potentials

$$\hat{H} = \frac{\hat{p}^2}{2m} + U; \quad \hat{H}' = \frac{\hat{p}^2}{2m} + U', \quad (3)$$

where  $m$  is a mass of the particle. In this section, we study the case of a short-range disorder, with the correlation length  $d \ll \lambda_0$ , which is essentially equivalent to a  $\delta$ -correlated (white-noise) random potential. Thus, we have the following expressions for the correlators:

$$\langle U(\mathbf{r}_1)U(\mathbf{r}_2) \rangle = \langle U'(\mathbf{r}_1)U'(\mathbf{r}_2) \rangle = \frac{1}{2\pi\nu\tau} \delta(\mathbf{r}_1 - \mathbf{r}_2), \quad (4)$$

where  $\tau$  is the mean free time (to simplify notations, we assume it to be exactly the same for  $U$  and  $U'$ ) and  $\nu$  is a density of states at the Fermi energy. The difference between the potentials  $\delta U = U' - U$  is characterized by another time scale  $\tilde{\tau}$ ,

$$\langle \delta U(\mathbf{r}_1)\delta U(\mathbf{r}_2) \rangle = \frac{1}{\pi\nu\tilde{\tau}} \delta(\mathbf{r}_1 - \mathbf{r}_2). \quad (5)$$

Clearly, we want to study the effect of a weak perturbation  $\delta U \ll U$  or, in the other words,  $\tilde{\tau} \gg \tau$ . Finally, we take the initial state  $|\psi\rangle$  in the form of a Gaussian wave packet

$$\psi(\mathbf{r}) = \left( \frac{1}{\pi\sigma^2} \right)^{D/4} \exp \left[ i\mathbf{p}_0 \cdot \mathbf{r} - \frac{\mathbf{r}^2}{2\sigma^2} \right], \quad (6)$$

where  $\sigma \gg \lambda_0 = 2\pi/p_0$  is a width of the packet and  $D$  is a number of space dimensions (we set  $\hbar = 1$  throughout the paper).

To translate (1) into the diagrammatic language, we represent the ensemble-averaged fidelity as an average product of four Green's functions

$$\begin{aligned} M(t) = & \int d\mathbf{r}_1 \cdots d\mathbf{r}_6 \langle \psi(\mathbf{r}_1) G^R(\mathbf{r}_1, \mathbf{r}_2; t) \\ & \times G^{A'}(\mathbf{r}_2, \mathbf{r}_3; -t) \psi^*(\mathbf{r}_3) \psi(\mathbf{r}_4) G^{R'}(\mathbf{r}_4, \mathbf{r}_5; t) \\ & \times G^A(\mathbf{r}_5, \mathbf{r}_6; -t) \psi^*(\mathbf{r}_6) \rangle, \end{aligned} \quad (7)$$

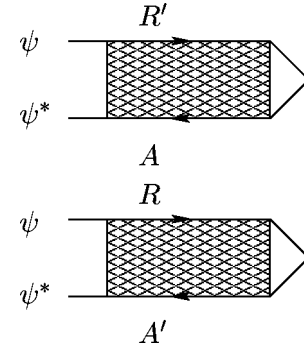


FIG. 1. Diagram determining the short-time (golden-rule) behavior of the fidelity.

where

$$G^{R,A} = \int \frac{dE}{2\pi} (E - \hat{H} \pm i0)^{-1} e^{-iEt},$$

$$G^{R',A'} = \int \frac{dE}{2\pi} (E - \hat{H}' \pm i0)^{-1} e^{-iEt}. \quad (8)$$

The diagrams are then obtained by connecting four lines representing the Green's functions in Eq. (7) via the diffusion ladders. At sufficiently short times the leading contribution is given by the simplest diagram shown in Fig. 1.

The solid lines in Fig. 1 correspond to the impurity-averaged Green's functions

$$\bar{G}^{R,A}(\epsilon, \mathbf{p}) = \bar{G}^{R',A'}(\epsilon, \mathbf{p}) = \frac{1}{\epsilon - \epsilon_p \pm i/2\tau}, \quad (9)$$

with  $\epsilon_p = p^2/2m$ , and the shaded box represents the diffuson (see Fig. 2),

$$\tilde{\Pi}(\mathbf{Q}, \omega) = \frac{1}{2\pi\nu\tau^2(DQ^2 - i\omega + 1/\tilde{\tau})}, \quad (10)$$

where  $D = v_0^2\tau/D$  is the diffusion coefficient and  $v_0 = p_0/m$ . Note that this diffuson has a nonzero ‘‘mass’’  $1/\tilde{\tau}$ , since it represents an averaged product of two Green's functions in different potentials  $\langle G^R G^{A'} \rangle$ . We will only need this diffuson for zero momentum  $\mathbf{Q}$  and integrated with two Green's functions, therefore it is convenient to introduce

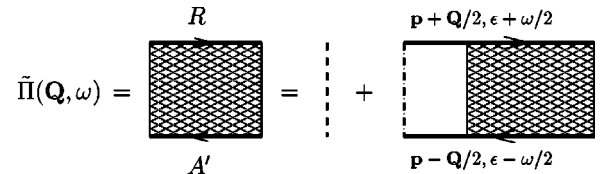


FIG. 2. Dyson equation for the ‘‘massive diffuson.’’ The dashed line corresponds to the correlator  $\langle UU' \rangle$ .

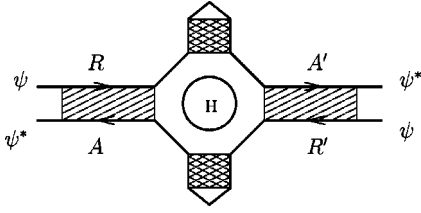


FIG. 3. Diagram determining the long-time diffusive asymptotics of  $M(t)$ .

$$\begin{aligned} \tilde{\Gamma}(\omega) &= \int \frac{d\mathbf{p}}{(2\pi)^D} G^R\left(\epsilon + \frac{\omega}{2}, \mathbf{p}\right) G^{A'}\left(\epsilon - \frac{\omega}{2}, \mathbf{p}\right) \tilde{\Pi}(\mathbf{0}, \omega) \\ &= \frac{1}{\tau(-i\omega + 1/\tilde{\tau})}. \end{aligned} \quad (11)$$

To shorten notations, we will also denote  $\bar{G}_{\psi}^{R,R'}(\epsilon, \mathbf{p}) = \psi(\mathbf{p})\bar{G}^{R,R'}(\epsilon, \mathbf{p})$  and  $\bar{G}_{\psi}^{A,A'}(\epsilon, \mathbf{p}) = \psi^*(\mathbf{p})\bar{G}^{A,A'}(\epsilon, \mathbf{p})$ , where  $\psi(\mathbf{p}) = (4\pi\sigma^2)^{D/4} e^{-i(\mathbf{p}-\mathbf{p}_0)^2\sigma^2/2}$  is the wave function in the momentum representation.

With the above definitions, the expression corresponding to the diagram Fig. 1 has the form

$$\begin{aligned} M(t) &= \left| \int \frac{d\mathbf{p}}{(2\pi)^D} \frac{d\epsilon d\epsilon'}{(2\pi)^2} e^{-i(\epsilon-\epsilon')t} \right. \\ &\quad \left. \times \bar{G}_{\psi}^R(\epsilon, \mathbf{p}) \tilde{\Gamma}(\epsilon-\epsilon') \bar{G}_{\psi}^{A'}(\epsilon', \mathbf{p}) \right|^2. \end{aligned} \quad (12)$$

After a straightforward calculation, we get the following result for the fidelity:

$$M(t) = e^{-2t/\tilde{\tau}}. \quad (13)$$

This is nothing but the golden-rule decay induced by the perturbation (5).

For long times  $t \gg \tilde{\tau}$  the contribution (13) becomes exponentially small in view of the massive character of the diffusons (10). The long-time behavior of the fidelity is, however, determined by a different diagram shown in Fig. 3, with two massive diffusons “colliding” and transforming into two conventional, massless diffusons (Fig. 4),

$$\Pi(\mathbf{Q}, \omega) = \frac{1}{2\pi\nu\tau^2} \frac{1}{DQ^2 - i\omega}. \quad (14)$$

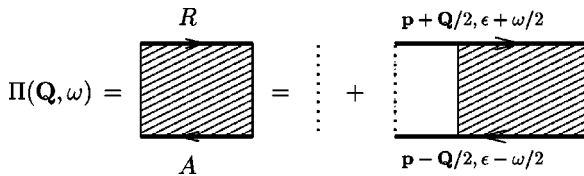


FIG. 4. Dyson equation for the conventional diffuson  $\Pi(\mathbf{Q}, \omega)$ . The dotted line corresponds to the correlator  $\langle UU \rangle = \langle U' U' \rangle$ .

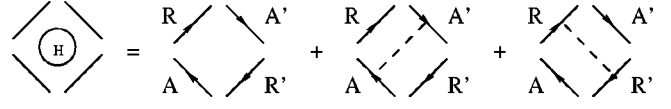


FIG. 5. Diffuson “collision” vertex (Hikami box).

The diffuson “collision” vertex, conventionally termed the Hikami box, is given by a sum of diagrams shown in Fig. 5, yielding

$$\chi(\mathbf{Q}, \epsilon - \epsilon') = \frac{4\pi\nu\tau^2}{\tilde{\tau}} \frac{1}{(\epsilon - \epsilon')^2 + (1/\tau)^2}. \quad (15)$$

Note the unconventional form of the expression for the Hikami box: due to  $\langle UU' \rangle \neq \langle UU \rangle$ , the diagrams in Fig. 5 do not cancel when all diffuson momenta and frequencies are equal to zero. Further, we neglected the momentum and frequencies of massless diffusons in Eq. (15); the corresponding terms will be smaller by a factor  $\tilde{\tau}/t \ll 1$ .

Combining everything, we thus get the following expression corresponding to the diagram in Fig. 3:

$$\begin{aligned} M(t) &= \int \frac{d\mathbf{p} d\mathbf{p}' d\mathbf{Q}}{(2\pi)^{3D}} \int \frac{d\epsilon d\epsilon' d\omega_1 d\omega_2}{(2\pi)^4} e^{-i(\omega_1 + \omega_2)t} \\ &\quad \times \bar{G}_{\psi}^R\left(\mathbf{p} - \frac{\mathbf{Q}}{2}, \epsilon + \frac{\omega_1}{2}\right) \bar{G}_{\psi}^A\left(\mathbf{p} + \frac{\mathbf{Q}}{2}, \epsilon - \frac{\omega_1}{2}\right) \\ &\quad \times \Pi(\mathbf{Q}, \omega_1) \chi(\mathbf{Q}, \epsilon - \epsilon') |\tilde{\Gamma}(\epsilon - \epsilon')|^2 \Pi(\mathbf{Q}, \omega_2) \\ &\quad \times \bar{G}_{\psi}^{A'}\left(\mathbf{p}' - \frac{\mathbf{Q}}{2}, \epsilon' - \frac{\omega_2}{2}\right) \bar{G}_{\psi}^{R'}\left(\mathbf{p}' + \frac{\mathbf{Q}}{2}, \epsilon' + \frac{\omega_2}{2}\right). \end{aligned} \quad (16)$$

Performing all the energy integrations, we get the following result:

$$\begin{aligned} M(t) &= \int \frac{d\mathbf{p} d\mathbf{p}' d\mathbf{Q}}{(2\pi)^{3D}} e^{-2DQ^2 t} e^{-Q^2\sigma^2/2} e^{-i(\mathbf{p}-\mathbf{p}_0)^2\sigma^2} \\ &\quad \times e^{-i(\mathbf{p}'-\mathbf{p}_0)^2\sigma^2} \frac{(4\pi\sigma^2)^D}{\pi\nu\tau} \frac{1}{(\epsilon_{\mathbf{p}} - \epsilon_{\mathbf{p}'})^2 + \frac{1}{\tau^2}}. \end{aligned} \quad (17)$$

Before writing down the final result, we should be more specific about the width  $\sigma$  of the original wave packet. When it is large compared to the mean free path,  $\sigma \gg v_0\tau$ , the characteristic deviations  $|\mathbf{p} - \mathbf{p}_0|$ ,  $|\mathbf{p}' - \mathbf{p}_0|$  are of the order of  $1/\sigma$  due to Gaussian factors, and we can set  $|\mathbf{p}| = |\mathbf{p}'|$  in the last factor in Eq. (17). In the opposite case  $\sigma \ll v_0\tau$ , the difference  $|\mathbf{p}| - |\mathbf{p}'|$  is of the order of  $1/(v_0\tau) \ll 1/\sigma$  and can be neglected in the above Gaussian factors. Thus, we have

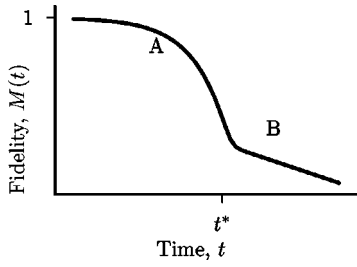


FIG. 6. Schematic representation of the time evolution of the Loschmidt echo  $M(t)$  for a white-noise disorder on a log-log plot: A, golden-rule exponential decay (13); B, diffusive power-law decay (18) and (19).

$$M(t) = \frac{v_0 \tau}{2\pi\sigma} \frac{\Gamma(D/2)}{(p_0 \sigma)^{D-1}} \left( \frac{2\sigma^2}{4Dt + \sigma^2} \right)^{D/2}, \quad \sigma \gg v_0 \tau, \quad (18)$$

$$M(t) = \frac{1}{2\sqrt{2\pi}} \frac{\Gamma(D/2)}{(p_0 \sigma)^{D-1}} \left( \frac{\sigma^2}{2Dt} \right)^{D/2}, \quad \sigma \ll v_0 \tau, \quad (19)$$

where  $\Gamma(x)$  is the Euler Gamma function. Remarkably, this large- $t$  behavior of the Loschmidt echo is independent of  $\tilde{\tau}$ , i.e., of the perturbation strength.

Therefore, the long-time asymptotic behavior of the fidelity is a power-law decay governed by the diffusion, with  $M(t)$  proportional to the inverse diffusion volume  $V_{\text{diff}} = (Dt)^{D/2}$ . Clearly, this result obtained from the diffusion diagram technique is not specific for the white-noise disorder considered in this section but rather yields a generic form of the long- $t$  behavior of  $M(t)$  in diffusive systems. Comparing the results (18) and (19) with contribution from (13), one can determine the time  $t^*$  of crossover between the exponential and the power-law regimes, which is larger than  $\tilde{\tau}$  by a logarithmic factor. In particular, for a two-dimensional system with  $\sigma < l$ , we have  $t^* = (\tilde{\tau}/2) \ln(p_0 D \tilde{\tau} / \sigma)$ . The behavior of  $M(t)$  for the case of a short-range potential studied in this section is illustrated schematically in Fig. 6.

We will now show that the result (19) can be obtained from classical arguments. Let us consider the classical fidelity introduced in Refs. [8,13,15,17] and defined as an overlap of two classical phase-space distribution functions

$$M_{\text{cl}}(t) = \int n(\mathbf{p}, \mathbf{r}, t) n'(\mathbf{p}, \mathbf{r}, t) \frac{d\mathbf{p} d\mathbf{r}}{(2\pi)^D}. \quad (20)$$

Here,  $n(\mathbf{p}, \mathbf{r}, t)$  is a distribution function obtained from the initial distribution  $n(\mathbf{p}, \mathbf{r}, 0)$  by the action of the classical evolution operator corresponding to the Hamiltonian  $\hat{H}$  and  $n'(\mathbf{p}, \mathbf{r}, t)$  is obtained by the evolution operator corresponding to the slightly perturbed Hamiltonian  $\hat{H}'$ . This quantity indeed possesses the properties of fidelity if the initial distribution is derived from a Wigner function  $W_\psi$  of a pure quantum mechanical state,  $n(\mathbf{p}, \mathbf{r}, 0) = W_\psi(\mathbf{p}, \mathbf{r}, 0)$ , implying, in particular,  $M_{\text{cl}}(0) = \int n^2(\mathbf{p}, \mathbf{r}, 0) d\mathbf{p} d\mathbf{r} / (2\pi)^D = 1$ . For the initial state (6), the corresponding Wigner function is

$$W_\psi(\mathbf{p}, \mathbf{r}) = 2^D e^{-\mathbf{r}^2/\sigma^2} e^{(\mathbf{p}-\mathbf{p}_0)^2 \sigma^2}. \quad (21)$$

The classical evolution of the coordinate part of  $n_\psi(\mathbf{p}, \mathbf{r}, t)$  is described by the diffusion propagator

$$\mathcal{P}(\mathbf{r}_1, \mathbf{r}_2, t) = \frac{1}{(4\pi Dt)^{D/2}} \exp\left(-\frac{(\mathbf{r}_1 - \mathbf{r}_2)^2}{4Dt}\right). \quad (22)$$

The final momentum distribution is uniform over the momentum direction, while the distribution of  $|\mathbf{p}|$  is determined by the energy conservation. Thus, we have

$$n_\psi(\mathbf{p}, \mathbf{r}, t) = \frac{1}{(4\pi Dt)^{D/2}} \exp\left(-\frac{\mathbf{r}^2}{4Dt}\right) \times \frac{(4\pi)^{(D-1)/2} \Gamma(D/2)}{p_0^{D-1}} \exp[-(|\mathbf{p}| - p_0)^2 \sigma^2], \quad (23)$$

where we assumed that the time  $t$  is sufficiently large,  $\sigma^2 \ll Dt$ . The difference between the Hamiltonians  $\hat{H}$  and  $\hat{H}'$  is insignificant for the diffusive dynamics, so that  $n'(\mathbf{p}, \mathbf{r}, t)$  is given by the same formula (23). Inserting the expression (23) for  $n$  and  $n'$  into Eq. (20), we get

$$M_{\text{cl}}(t) = \int n^2(\mathbf{p}, \mathbf{r}, t) \frac{d\mathbf{p} d\mathbf{r}}{(2\pi)^D} = \frac{1}{2\sqrt{2\pi}} \frac{\Gamma(D/2)}{(p_0 \sigma)^{D-1}} \left( \frac{\sigma^2}{2Dt} \right)^{D/2}, \quad (24)$$

which is identical to the result (19) of the quantum mechanical calculation.

The result (19) differs from Eq. (24) by the prefactor  $v_0 \tau / \sigma$ . This can be understood if we take into account that for  $\sigma \gg l = v_0 \tau$  the width of the distribution of  $|\mathbf{p}|$  is determined by the quantum uncertainty of the momentum  $\delta|\mathbf{p}| \sim l^{-1}$  rather than by  $\sigma^{-1}$  as in the classical formula (23).

We see that the long-time behavior of the classical (20) and quantum (1) fidelity is essentially the same. This agrees with the results of numerical study of a quantum chaotic system (the sawtooth map) in Ref. [8].

In low-dimensional systems,  $D \leq 2$ , the behavior of the quantum fidelity is affected at very long times by the quantum localization effects (which have been neglected in our considerations). These effects will lead to a saturation of the quantum fidelity at the time  $t_{\text{loc}} \sim L_{\text{loc}}^2 / D$ , where  $L_{\text{loc}}$  is a localization length. Specifically, for a quasi-one-dimensional system  $t_{\text{loc}} \sim v^2 D$  and for a two-dimensional system  $t_{\text{loc}} \sim \tau e^{4\pi^2 v D}$ .

It is worth mentioning that our diagrammatic calculation bears a certain similarity to earlier studies of intensity fluctuations and correlations for waves propagating in random media [24–26]. In particular, sensitivity of transport quantities to a small change of the impurity potential (e.g., due to a displacement of a single-scattering center) has been investigated [27,24]. However, the Loschmidt echo is essentially

different from the quantities studied in these papers since it involves propagation in two different potentials  $U$ ,  $U'$  already before the ensemble averaging. Formally, this corresponds to switching between the Green's functions  $G$  and  $G'$  in external vertices (see Figs. 1 and 3).

### III. LOSCHMIDT ECHO FOR THE LONG-RANGE POTENTIAL

After having understood the behavior of the fidelity in a white-noise disorder, we turn to the case of our main interest, a long-range potential with a correlation length  $d \gg \lambda_0$ . For this kind of potential, the characteristic angle of diffraction for each scattering event is small,  $\delta\phi \sim \lambda_0/d$ , so that many scattering events are needed to change strongly the velocity direction. As a result, the motion in such a disorder is characterized by two relaxation times. The first one is the quantum (or, in another terminology, single-particle) relaxation time  $\tau_s$ , which is the mean time between scattering events. This time determines the decay rate of the averaged Green's function  $\langle G^R(\mathbf{r}, t) \rangle = G_0^R(\mathbf{r}, t) e^{-t/2\tau_s}$ . The second one, the momentum (or, transport) relaxation time  $\tau_{tr}$  sets the time scale on which the velocity direction changes by an angle of the order of  $\pi$ . It is parametrically larger,  $\tau_{tr} \sim (d/\lambda_0)^2 \tau_s$ . The transport time determines, in particular, the diffusion coefficient  $\mathcal{D} = v_0^2 \tau_{tr}/D$ .

The condition (2) implies that in the diagrammatic approach the leading contribution is given by diagrams with noncrossing impurity lines. In particular,  $\tau_s$  is determined by the Born-approximation self-energy diagram,  $\tau_{tr}$  is obtained by taking into account the ladder-type vertex correction, and the diffusion propagator can be calculated by solving the

equation corresponding to the sum of the ladder diagrams [28]. Furthermore, even in the ballistic range of frequency and momenta  $q l_{tr} > 1$ ,  $\omega \tau_{tr} > 1$ , the average product of two Green's functions  $\langle G_R G_A \rangle$  is determined by a sum of ladder diagrams, the "ballistic diffuson." One might thus expect that the diagrammatic calculation of the preceding section can be generalized to the case of a long-range disorder. Indeed, both the golden-rule short-time behavior corresponding to Fig. 1 and the long-time diffusion power-law asymptotics determined by the diagram of Fig. 3 do retain their validity for a long-range disorder. However, as we demonstrate below, an intermediate time range emerges, where the diagrammatic approach is not applicable. The reason for this is a necessity to average a product of four Green's functions describing four electronic trajectories propagating close to each other. As was shown in Ref. [23], in a certain time range (specified below) these four Green's functions do not decouple into two (ballistic) diffusons, but rather are coupled all together by impurity correlators into a more complicated object, a "four-diffuson." In view of the failure of the ballistic-diffuson diagrammatics, we will use the path-integral approach developed in Refs. [29,23]. For simplicity, we consider a two-dimensional system.

We begin by defining the disorder correlation functions [replacing the white-noise formulas (4) and (5)]

$$\langle U(\mathbf{r}) U(\mathbf{r}_1) \rangle = \langle U'(\mathbf{r}) U'(\mathbf{r}_1) \rangle = W(|\mathbf{r} - \mathbf{r}_1|),$$

$$\langle \delta U(\mathbf{r}) \delta U(\mathbf{r}_1) \rangle = 2 \delta W(|\mathbf{r} - \mathbf{r}_1|). \quad (25)$$

Introducing the Feynman path-integral representation and averaging over the disorder, we rewrite the product of four Green's functions in Eq. (7) as

$$\begin{aligned} & \langle G_R(\mathbf{R}_1, \mathbf{R}_2, T) G_{A'}(\mathbf{R}_2, \mathbf{R}_3, -T) G_{R'}(\mathbf{R}_4, \mathbf{R}_5, T) G_A(\mathbf{R}_5, \mathbf{R}_6, -T) \rangle \\ &= \int_{\mathbf{r}_1(0)=\mathbf{R}_1}^{\mathbf{r}_1(T)=\mathbf{R}_2} \int_{\mathbf{r}_3(0)=\mathbf{R}_2}^{\mathbf{r}_3(T)=\mathbf{R}_3} \int_{\mathbf{r}_2(0)=\mathbf{R}_4}^{\mathbf{r}_2(T)=\mathbf{R}_5} \int_{\mathbf{r}_4(0)=\mathbf{R}_5}^{\mathbf{r}_4(T)=\mathbf{R}_6} \prod_{i=1}^4 \mathcal{D}\mathbf{r}_i \exp[iS_{\text{kin}} - S_W], \end{aligned} \quad (26)$$

$$S_{\text{kin}} = \frac{m}{2} \int_0^T dt (\dot{\mathbf{r}}_1^2 + \dot{\mathbf{r}}_2^2 - \dot{\mathbf{r}}_3^2 - \dot{\mathbf{r}}_4^2),$$

$$S_W = \frac{1}{2} (S_{11} + S_{22} + S_{33} + S_{44}) + S_{12} + S_{34} - S_{13} - S_{14} - S_{23} - S_{24} - \delta S_{12} - \delta S_{34} + \delta S_{13} + \delta S_{24},$$

$$S_{ij} = \int_0^T \int_0^T W(\mathbf{r}_i(t) - \mathbf{r}_j(t')) dt dt',$$

$$\delta S_{ij} = \int_0^T \int_0^T \delta W(\mathbf{r}_i(t) - \mathbf{r}_j(t')) dt dt', \quad (27)$$

where the paths  $\mathbf{r}_1, \mathbf{r}_2$  correspond to the retarded and  $\mathbf{r}_3, \mathbf{r}_4$  to the advanced Green's functions. The path integral (26) is similar to the one evaluated in Ref. [23], a difference being in boundary conditions and in the additional terms  $\delta S_{ij}$  in the action induced by the perturbation  $\delta U$ . As in Ref. [23], it is useful to perform the change of variables, introducing  $\mathbf{R}_+ = (\mathbf{r}_1 + \mathbf{r}_2 + \mathbf{r}_3 + \mathbf{r}_4)/4$ ,  $\mathbf{R}_- = (\mathbf{r}_1 + \mathbf{r}_2 - \mathbf{r}_3 - \mathbf{r}_4)$ ,  $\mathbf{r}_+ = (\mathbf{r}_1 - \mathbf{r}_2 + \mathbf{r}_3 - \mathbf{r}_4)/2$ ,  $\mathbf{r}_- = (\mathbf{r}_1 - \mathbf{r}_2 - \mathbf{r}_3 + \mathbf{r}_4)/2$ . The boundary conditions in terms of the new variables are as follows. At  $t = T$ , we have  $\mathbf{R}_-(T) = 0$  and  $\mathbf{r}_-(T) = 0$ , while the integration over  $\mathbf{R}_+(T)$  and  $\mathbf{r}_+(T)$  are unrestricted. At  $t = 0$  the integration over  $\mathbf{R}_\pm(0)$  and  $\mathbf{r}_\pm(0)$  is performed with the weight

$$\psi(\mathbf{R}_1)\psi^*(\mathbf{R}_3)\psi(\mathbf{R}_4)\psi^*(\mathbf{R}_6) = \left(\frac{1}{\pi\sigma^2}\right)^2 \exp\left\{-\frac{4\mathbf{R}_+(0)^2 + \mathbf{R}_-^2(0)/4 + \mathbf{r}_+(0)^2 + \mathbf{r}_-(0)^2}{2\sigma^2} + i\mathbf{p}_0\mathbf{R}_-(0)\right\}. \quad (28)$$

The kinetic part of the action reads in the transformed variables as

$$S_{\text{kin}} = m \int_0^T dt (\dot{\mathbf{r}}_+ \dot{\mathbf{r}}_- + \dot{\mathbf{R}}_+ \dot{\mathbf{R}}_-). \quad (29)$$

As was shown in Ref. [23], the pairs of variables  $(\mathbf{R}_+, \mathbf{R}_-)$  and  $(\mathbf{r}_+, \mathbf{r}_-)$  decouple. On ballistic distances  $\ll l_{\text{tr}}$ , the integral over the first pair is essentially of the free-particle type, and its saddle-point yields the classical equation of motion for the ‘‘center of mass’’ coordinate  $\mathbf{R}_+$ ,

$$\mathbf{R}_+(t) = \mathbf{R}_+(0) + [\mathbf{R}_+(T) - \mathbf{R}_+(0)] \frac{t}{T}. \quad (30)$$

After integrating out  $\mathbf{R}_+, \mathbf{R}_-$ , the action (29) is reduced to the form

$$S_{\text{kin}} = m \frac{\mathbf{R}_+(T) - \mathbf{R}_+(0)}{2T} [\mathbf{R}_-(T) - \mathbf{R}_-(0)] + m \int_0^T dt \dot{\mathbf{r}}_+ \dot{\mathbf{r}}_-. \quad (31)$$

Since we are interested in the ballistic scales ( $\ll l_{\text{tr}}$ ), it is convenient to split  $\mathbf{R}_-, \mathbf{r}_+, \mathbf{r}_-$  into components parallel  $\parallel$  and perpendicular  $\perp$  to the direction of the motion  $\dot{\mathbf{R}}_+$ . Then the disorder-induced part of the action  $S_{\text{W}}$  depends only on the transverse components  $\mathbf{R}_{-\perp}$  and  $\mathbf{r}_{\pm\perp}$ , which we will denote  $Y_-$  and  $\rho_{\pm}$ , respectively,

$$S_{\text{W}} \simeq \int_0^T \mathcal{U}(\rho_-(t), \rho_+(t)) dt - 2 \int_0^T dt Y_-^2(t) \{G(\rho_-(t)) - \delta G(\rho_-(t)) + G(\rho_+(t))\}, \quad (32)$$

where

$$\mathcal{U} = \mathcal{U}_0 + \delta\mathcal{U},$$

$$\mathcal{U}_0 = 2[F(\rho_+) + F(\rho_-)] - F(\rho_+ + \rho_-) - F(\rho_+ - \rho_-),$$

$$\delta\mathcal{U} = -2\delta F(\rho_-) + \delta F(\rho_+ + \rho_-) + \delta F(\rho_+ - \rho_-), \quad (33)$$

and we have introduced the functions

$$F(y) \equiv \int_0^{\infty} \frac{dx}{v_0} [W(x,0) - W(x,y)],$$

$$\delta F(y) \equiv \int_0^{\infty} \frac{dx}{v_0} [\delta W(x,0) - \delta W(x,y)], \quad (34)$$

$$G(y) \equiv \int_0^{\infty} \frac{dx}{v_0} \frac{\partial^2}{\partial y^2} W(x,y),$$

$$\delta G(y) \equiv \int_0^{\infty} \frac{dx}{v_0} \frac{\partial^2}{\partial y^2} \delta W(x,y). \quad (35)$$

Since the correlation functions  $W(r)$ ,  $\delta W(r)$  decay on the scale  $d$ , the functions  $F$ ,  $G$ ,  $\delta F$ , and  $\delta G$  have the following asymptotic behavior:  $F(y \ll d) \simeq -G(0)y^2/2$ ,  $F(y \gg d) \simeq \tau_s^{-1}$ ,  $G(0) = -m^2 v_0^2 / \tau_{\text{tr}}$ , and  $G(y \gg d) \rightarrow 0$ , and analogously  $\delta F(y \ll d) \simeq -\delta G(0)y^2/2$ ,  $\delta F(y \gg d) \simeq \tilde{\tau}_s^{-1}$ ,  $\delta G(0) = -m^2 v_0^2 / \tilde{\tau}_{\text{tr}}$ ,  $\delta G(y \gg d) \rightarrow 0$ . Here, the times  $\tau_s$  and  $\tau_{\text{tr}}$  are defined according to

$$\frac{1}{\tau_s} = \frac{2}{v_0} \int_0^{\infty} W(r) dr, \quad (36)$$

$$\frac{1}{\tau_{\text{tr}}} = -\frac{1}{m^2 v_0^3} \int_0^{\infty} \frac{dr}{r} \frac{dW(r)}{dr}. \quad (37)$$

As shown in Ref. [29], these are exactly the expressions for the single particle and the transport times in a long-range disorder. The times  $\tilde{\tau}_s$  and  $\tilde{\tau}_{\text{tr}}$  are defined by the equations analogous to Eqs. (36) and (37) but with a substitution  $W \rightarrow \delta W$ .

Taking into account the boundary conditions (28) and integrating out the variables  $\mathbf{R}_{\pm}$ , we get the following expression for the fidelity:

$$M(T) = \int \frac{d\rho_+ d\rho_-}{\sqrt{2\pi\sigma^2}} e^{-(\rho_-^2 + \rho_+^2)/2\sigma^2} g(\rho_+, \rho_-; T). \quad (38)$$

The function  $g$  entering (38) is determined by the  $\rho_{\pm}$  part of the path integral, which can be reduced in the standard way to a differential equation:

$$\left(\frac{\partial}{\partial t} - \frac{i}{m} \frac{\partial^2}{\partial \rho_+ \partial \rho_-} + \mathcal{U}(\rho_+, \rho_-)\right) g(\rho_+, \rho_-, t) = \delta(t) \delta(\rho_-). \quad (39)$$

The left-hand-side of this equation reduces to that of Eq. (36) in Ref. [23] if the forward and backward evolution are performed in the same potential,  $\delta\mathcal{U} = 0$  (the right-hand-side differs from Ref. [23] because of different boundary conditions). The presence of  $\delta\mathcal{U}$  [which enters the ‘‘potential energy’’  $\mathcal{U}$ , see Eq. (33)] in Eq. (39) is crucially important: otherwise the solution would be simply  $g(\rho_+, \rho_-, t) = \delta(\rho_-)$  for any  $t > 0$ , since the boundary condition in Eq. (39) is independent of  $\rho_+$  and  $\mathcal{U}_0(\rho_+, 0) = 0$ . After a substitution into Eq. (38), this would lead to  $M(t) = 1$ , which is the correct result in the absence of perturbation.

We have therefore reduced the problem of calculation of the Loschmidt echo in the ballistic time range to a solution of the kinetic equation (39). Let us consider the time evolution of the solution of Eq. (39). The initial value at  $t \rightarrow 0$  is  $g = \delta(\rho_-)$ , and as explained above, the time evolution is initially determined by the term  $\delta\mathcal{U}$  that induces a  $\rho_+$  dependence of the solution. As a result, the distribution  $g$  becomes quickly suppressed at  $\rho_+ \geq d$  because

$$\delta\mathcal{U}(\rho_+, 0) \simeq \frac{2}{\tau_s}, \quad \rho_+ \gg d. \quad (40)$$

Thus, for  $\rho_+ \gg d$  Eq. (39) reduces to

$$\frac{\partial}{\partial t} g + \frac{2}{\tau_s} g = 0, \quad (41)$$

which gives an exponential decay

$$g \simeq \begin{cases} \delta(\rho_-), & \rho_+ \ll d \\ \delta(\rho_-) e^{-2t/\tau_s}, & \rho_+ \gg d. \end{cases} \quad (42)$$

Therefore, for  $t \gg \tilde{\tau}_s$ , the function  $g$  remains essentially non-vanishing only in the region  $\rho_+, \rho_- \ll d$ . In this region, we can expand  $\mathcal{U}$  up to the leading terms in  $\rho_+$  and  $\rho_-$  and rewrite Eq. (39) in the form

$$\left( \frac{\partial}{\partial t} - \frac{i}{m} \frac{\partial^2}{\partial \rho_+ \partial \rho_-} + \frac{m^2}{\tau_L^3} \rho_+^2 \rho_-^2 + \frac{2m^2 v_0^2}{\tau_{tr}} \rho_+^2 \right) g = 0. \quad (43)$$

We have introduced here a time scale

$$\tau_L = \left[ \frac{3}{2m^2 v_0} \int_0^\infty \frac{dr}{r} \frac{d}{dr} \left( \frac{1}{r} \frac{dW(r)}{dr} \right) \right]^{-1/3} \sim \tau_{tr} \left( \frac{d}{l_{tr}} \right)^{2/3}. \quad (44)$$

As discussed below,  $\tau_L$  is equal (up to a numerical coefficient) to the inverse Lyapunov exponent in the corresponding classical problem, and we will call it the Lyapunov time.

At the early stage of the evolution, characteristic values of  $\rho_-$  are small, and the  $\rho_+^2 \rho_-^2$  term in Eq. (43) is small compared to the  $\rho_-^2$  term. More specifically, at  $t \sim \tilde{\tau}_s$ , we have  $\rho_- \sim \tilde{l}_s / (p_0 d)$ , so that the condition for neglecting the quartic term in this time range is  $l_L \gg \tilde{l}_s$ , where  $l_L = v_0 \tau_L$  is the Lyapunov length. We will assume in the sequel that this condition is fulfilled [30]. Thus, Eq. (39) reduces to

$$\left( \frac{\partial}{\partial t} - \frac{i}{m} \frac{\partial^2}{\partial \rho_+ \partial \rho_-} + \frac{2m^2 v_0^2}{\tau_{tr}} \rho_+^2 \right) g = 0. \quad (45)$$

Performing further a Fourier transformation  $\rho_+ \rightarrow i(mv_0)^{-1} \partial / \partial \phi$ ,  $\partial / \partial \rho_+ \rightarrow imv_0 \phi$ , we cast Eq. (39) into the following form:

$$\left( \frac{\partial}{\partial t} + v_0 \phi \frac{\partial}{\partial \rho_-} - \frac{2}{\tau_{tr}} \frac{\partial^2}{\partial \phi^2} \right) g = 0. \quad (46)$$

Remarkably, Eq. (46) has a meaning of the Boltzmann kinetic equation for the phase-space distribution function describing the motion in the transverse direction characterized by the coordinate  $\rho_-$ , with  $v_0 \phi$  playing the role of the corresponding velocity. This clarifies the meaning of  $\phi$  (and explains the notation); it is the angle the velocity vector makes with the  $\parallel$  axis. (We remind the reader that we are considering ballistic time scales, so that  $\phi \ll 1$ .) The last term in Eq. (46) plays the role of a collision integral and describes a diffusion process for the velocity angle. The solution of this equation is a Gaussian packet

$$g(\phi, \rho_-) = \frac{\sqrt{3} \tilde{\tau}}{2m v_0^2 t^2} \exp \left\{ \left( \frac{3\phi \rho_-}{v_0 t} - \frac{3\rho_-^2}{(v_0 t)^2} - \phi^2 \right) \frac{\tilde{\tau}}{2t} \right\}.$$

Transforming back to the variable  $\rho_+$ , we get

$$g(\rho_+, \rho_-) = \frac{1}{\sqrt{\pi \Sigma_-}} \exp \left\{ -\frac{\rho_-^2}{\Sigma_-} - \frac{\rho_+^2}{\Sigma_+} + 2i\sqrt{3} \frac{\rho_+ \rho_-}{\Sigma_+ \Sigma_-} \right\},$$

where

$$\begin{aligned} \Sigma_-(t) &= \frac{2v_0 t}{\sqrt{3}} \left( \frac{2t}{\tilde{\tau}_{tr}} \right)^{1/2}, \\ \Sigma_+(t) &= \frac{2}{mv_0} \left( \frac{\tilde{\tau}_{tr}}{2t} \right)^{1/2}. \end{aligned} \quad (47)$$

For the phase-space distribution function  $g(\phi, \rho_-)$  the quantities  $\Sigma_-$  and  $\Sigma_+^{-1}$  play the role of widths of the distribution with respect to the coordinate  $\rho_-$  and the momentum  $mv_0 \phi$ , respectively.

To simplify calculations, we will neglect the cross correlations between  $\rho_+$  and  $\rho_-$  [this will only influence a numerical prefactor in  $M(t)$ , which is of minor importance here] and assume that  $g$  has the form

$$g(\rho_+, \rho_-) = \frac{1}{\sqrt{\pi \Sigma_-}} \exp \left\{ -\frac{\rho_-^2}{\Sigma_-} - \frac{\rho_+^2}{\Sigma_+} \right\}. \quad (48)$$

We will see that this form of  $g$  will preserve during the further evolution of the distribution.

The characteristic values of  $\rho_-$  are increasing proportionally to  $t^{3/2}$ . Eventually, the neglected third (quartic) term in Eq. (43) becomes comparable to the fourth one. Using the result (47) for the characteristic value  $\Sigma_-(t)$  of  $\rho_-$ , it is easy to see that this happens at  $t = \tau_L$ . At  $t > \tau_L$  the fourth term dominates, and Eq. (43) takes the form

$$\left( \frac{\partial}{\partial t} - \frac{i}{m} \frac{\partial^2}{\partial \rho_+ \partial \rho_-} + \frac{m^2}{\tau_L^3} \rho_+^2 \rho_-^2 \right) g = 0. \quad (49)$$

After the Fourier transformation from  $\rho_+$  to  $\phi$ , the last term takes the form  $-(\rho_-^2 / v_0^2 \tau_L^3) \partial^2 g / \partial \phi^2$  and describes a diffusion process for the angle  $\phi$  with the diffusion coefficient proportional to the coordinate  $\rho_-$ . This is exactly the kinetic equation for the disorder-averaged distribution func-

tion  $g(\phi, \rho_-)$  of phase-space separations between two classical paths [19,23]. It leads to an exponential increase of the width of the distribution function  $g(\rho_-, \phi)$  with a rate given by the Lyapunov exponent  $\sim \tau_L^{-1}$ . Thus, in this Lyapunov regime, we have

$$\begin{aligned}\Sigma_-(t) &\approx v_0 \tau_L \left( \frac{\tau_L}{\tilde{\tau}_{\text{tr}}} \right)^{1/2} \exp \left\{ c \frac{t}{\tau_L} \right\}, \\ \Sigma_+(t) &\approx \lambda_0 \left( \frac{\tilde{\tau}_{\text{tr}}}{\tau_L} \right)^{1/2} \exp \left\{ -c \frac{t}{\tau_L} \right\},\end{aligned}\quad (50)$$

where  $c$  is a numerical coefficient of the order of unity.

Since Eq. (43) turns after the Fourier transform  $\rho_+ \rightarrow i(mv_0)^{-1} \partial/\partial\phi$  into a kinetic equation for the classical distribution function, in a long-range potential the classical fidelity (20) behaves in the same way as the quantum one for  $t \gg \tilde{\tau}_s$ . Let us emphasize a highly nontrivial character of the emergence of a classical kinetic equation. Indeed, we consider a random potential for which each scattering act is of a quantum (diffractive) nature and cannot be described classically. It is only after the disorder averaging that the classical kinetics is restored.

The Lyapunov regime breaks down when the width  $\Sigma_-$  reaches the correlation length  $d$ , i.e., at

$$\tau_E^* = (\tau_L/c) \ln(\tilde{\tau}_{\text{tr}}/\tau_{\text{tr}}). \quad (51)$$

This time plays a role analogous to the Ehrenfest time but only depends on classical parameters (if one assumes that the perturbation  $\delta U$  is independent of  $\hbar$ ). An analogous expression for the crossover time between the Lyapunov regime and the power-law regime (discussed below) was obtained in Ref. [13] for the classical fidelity in a different model (saw-tooth map).

When  $t > \tau_E^*$ , so that  $\rho_- \gg d$ , we can use another asymptote of the ‘‘potential’’  $\mathcal{U}(\rho_+, \rho_-)|_{\rho_- \gg d} = 2m^2 v_0^2 \rho_+^2 / \tau_{\text{tr}}$ . This leads to an equation very similar to Eq. (45) but with  $\tilde{\tau}_{\text{tr}}$  replaced by  $\tau_{\text{tr}}$ . Therefore, in analogy with Eq. (47), we have again a power-law dependence of the distribution widths,

$$\begin{aligned}\Sigma_-(t) &\approx v_0 t \left( \frac{t}{\tau_{\text{tr}}} \right)^{1/2}, \\ \Sigma_+(t) &\approx \lambda_0 \left( \frac{\tau_{\text{tr}}}{t} \right)^{1/2}.\end{aligned}\quad (52)$$

For times larger than  $t_E^*$  all the calculations can also be performed using the diagrammatic technique for ballistic systems. This is because four trajectories, which were coupled all together into a four-diffuson by disorder correlations in the Lyapunov regime, split now in two conventional ballistic diffusons separated by a distance  $\gg d$  [19,23].

Having obtained the solution  $g$  of the kinetic equation in all the regimes of interest, we can calculate the fidelity  $M(t)$ . Substituting Eq. (48) into Eq. (38), we get

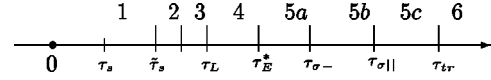


FIG. 7. Characteristic time scales separating various regimes of the behavior of  $M(t)$ . The regimes 2 (golden rule) and 4 (Lyapunov) correspond to an exponential decay of  $M(t)$ , the remaining regimes to a power-law decay (see text for details).

$$M(T) \approx \frac{\min(\Sigma_+(T), \sigma)}{\max(\Sigma_-(T), \sigma)}. \quad (53)$$

Thus, two additional time scales may become significant when we consider the fidelity:  $\tau_{\sigma+}$ , which is defined by  $\Sigma_+(\tau_{\sigma+}) = \sigma$  and  $\tau_{\sigma-}$  defined by  $\Sigma_-(\tau_{\sigma-}) = \sigma$ . Position of these time scales with respect to main characteristic times ( $\tau_L$ ,  $\tau_E^*$ ,  $\tau_{\text{tr}}$ ) depends on the width  $\sigma$  of the initial state. As an example, we choose  $d < \sigma < l_{\text{tr}}$ . In this case,  $\Sigma_+ < \sigma$  for all times  $t > \tilde{\tau}_s$ , so that the scale  $\tau_{\sigma+}$  does not arise, and  $\tau_E^* < \tau_{\sigma-} < \tau_{\text{tr}}$ . The order of all characteristic scales on the time axis is illustrated in Fig. 7.

We mention for completeness that there is one more characteristic time  $\tau_{\sigma||}$  located between  $\tau_{\sigma-}$  and  $\tau_{\text{tr}}$ . At this time, the approximation (30) of straight motion in the coordinate  $\mathbf{R}_+$  loses its validity. This leads to an additional factor  $\sigma/\max\{\sigma, \Sigma_{||}\}$  in the expression for  $M(t)$ , where

$$\Sigma_{||} \approx v t \frac{t}{\tau_{\text{tr}}} \quad (54)$$

characterizes longitudinal fluctuations of  $\mathbf{R}_+$ . There is thus an additional crossover inside the ballistic-diffusivity regime, which takes place at a time  $\tau_{\sigma||}$  satisfying  $\Sigma_{||}(\tau_{\sigma||}) = \sigma$ .

We are now prepared to summarize the results of this section and to give a list of all the regimes of behavior of the fidelity. We have found as much as six essentially different regimes (as illustrated in Fig. 7), one of them (the ballistic diffusion) splits up into three subregimes with different power-law behavior. We list the regimes in the order they appear as the time increases.

(1) Perfect echo regime,  $t \ll \tilde{\tau}_s$ . At such short times the perturbation is essentially irrelevant, and  $M(t) \approx 1$ .

(2) Golden-rule regime,  $t < \tilde{\tau}_s \ln(\sigma/d)$ . Substituting Eq. (42) into Eq. (38), we get the exponential decay

$$M(t) = e^{-2t/\tilde{\tau}_s}. \quad (55)$$

(3) Power-law ‘‘pre-Lyapunov inflation’’ regime,  $\tilde{\tau}_s \ln(\sigma/d) < t < \tau_L$ . Substituting Eq. (47) into Eq. (53), we get

$$M(t) \sim \frac{d}{\sigma} \left( \frac{\tilde{\tau}_s}{t} \right)^{1/2}. \quad (56)$$

This behavior of the fidelity is related to a power-law spreading of classical trajectories in this regime due to the ballistic diffusion in the perturbation potential  $\delta U$ .



(4) Lyapunov regime,  $\tau_L < t < \tau_E^*$ . Combining Eqs. (50) and (53), we get an exponential decay of the Loschmidt echo determined by the classical Lyapunov exponent

$$M(t) \sim \frac{d}{\sigma} \left( \frac{\tilde{\tau}_s}{\tau_L} \right)^{1/2} e^{-ct/\tau_L}. \quad (57)$$

(5) Ballistic diffusion regime,  $\tau_E^* < t < \tau_{tr}$ . This regime characterized by a power-law behavior of the fidelity is further subdivided into three subregimes.

(a)  $\tau_E^* < t < \tau_{\sigma-}$ . Using Eqs. (53) and (52) and noticing that  $\tilde{\Sigma}_-$  is still smaller than  $\sigma$  in this time range, we find

$$M(t) \sim \frac{1}{p_0 \sigma} \left( \frac{\tau_{tr}}{t} \right)^{1/2}. \quad (58)$$

(b)  $\tau_{\sigma-} < t < \tau_{\sigma||}$ . The only difference compared to the previous case is that now  $\tilde{\Sigma}_- > \sigma$ , yielding

$$M(t) \sim \frac{1}{p_0 l_{tr}} \left( \frac{\tau_{tr}}{t} \right)^2. \quad (59)$$

(c)  $\tau_{\sigma||} < t < \tau_{tr}$ . In this regime fluctuations in the motion in the parallel direction also become important, see the text around Eq. (54), with the result

$$M(t) \sim \frac{\sigma}{p_0 l_{tr}^2} \left( \frac{\tau_{tr}}{t} \right)^4. \quad (60)$$

(6) Conventional diffusion regime,  $t > \tau_{tr}$ . In this regime, the nature of disorder (short range vs long range) is irrelevant, and the result (18) derived in Sec. II is applicable,

$$M(t) \sim \frac{\sigma}{p_0 l_{tr}^2} \frac{\tau_{tr}}{t}. \quad (61)$$

We would like to remind the reader that the ordering of relevant time scales in Fig. 7 depends on the microscopic parameters of the problem. We have considered the most interesting case ( $\tilde{l}_s \ll l_L$  and  $d < \sigma < l_{tr}$ ), when all possible regimes are developed. For other choices of parameters, some of the regimes may disappear (see, in particular, Ref. [30]).

#### IV. CONCLUSIONS

In this paper, we have studied the Loschmidt echo (or, in a different terminology, the fidelity), which characterizes the sensitivity of a quantum system to an external perturbation, in a model with a weak quantum random potential. Using the diagrammatic approach, we have shown that at short times the fidelity decays exponentially with the rate  $2/\tilde{\tau}_s$  set by the golden rule, while its long-time asymptotics is of power-law type and is determined by the diffusive nature of the dynamics on this time scale. For a sufficiently long-range disorder a time range emerges where the diagrammatics becomes inapplicable due to merging of two ballistic diffusons into a more complicated four-diffuson. To study the fidelity in this regime, we have applied a quasiclassical (path-integral) ap-

proach. This allowed us to express the disorder-averaged fidelity in terms of a solution of a quasiclassical evolution equation, see Eqs. (38) and (39). On time scales larger than  $\tilde{\tau}_s$ , this equation takes a form of the kinetic equation for the distribution function  $g(\phi, \rho_-)$  of phase-space separations between two *classical* paths (one of which is subject to the perturbation). Solving the kinetic equation, we find several additional regimes of behavior of the Loschmidt echo, separating the short-time golden-rule decay from the long-time diffusive asymptotics. In particular, there arises a ‘‘Lyapunov regime,’’ where the fidelity decays exponentially with a rate governed by the classical Lyapunov exponent.

Therefore, apart from the short-time golden-rule regime, the behavior of the fidelity turns to be by and large classical; the quantum fidelity (1) follows essentially the classical one (20). This quantum-classical correspondence is limited, on the side of very long times, by quantum localization effects (leading to saturation of quantum fidelity). Our analytical findings corroborate numerical results of Ref. [8], where an almost identical behavior of  $M(t)$  and  $M_{cl}(t)$  for a chaotic map was observed.

It is worth mentioning that our path-integral calculation of the fidelity is closely connected to the analysis of quantum interference effects in a long-range disorder performed in Refs. [19,23]. In particular, after the Fourier transformation  $\rho_+ \rightarrow \phi$  our evolution equation (43) has the same form as the equation describing the Hikami box in Ref. [19] (after averaging over the smooth random potential). This is a remarkable agreement, since the methods used are essentially different: Aleiner and Larkin [19] work in a given realization of a random potential [which assumes that the potential is classical, i.e., the condition opposite to Eq. (2) is fulfilled], while we consider the case of a diffractive scattering [Eq. (2)] and perform all calculations for disorder-averaged quantities. There is, however, an important difference between the equations obtained. Specifically, in our case the last term of Eq. (43) (which is proportional to  $1/\tilde{\tau}_{tr}$ ) is due to the difference  $\delta U$  between the Hamiltonians for the forward and the backward propagation. On the other hand, the authors of Ref. [19] add ‘‘by hand’’ a term of exactly the same type (with a certain time  $\tau_q$  replacing our  $\tilde{\tau}_{tr}$ ) for a problem without any perturbation  $\delta U$ , arguing that it mimics a small-angle diffraction in the system. To our opinion, this justification is questionable (at least, for a system with a weak smooth disorder). Indeed, in this case all scattering processes determining the transport in the system are of diffractive type and are taken into account in our approach. There is thus no freedom to add an additional ‘‘diffractive’’ term to the kinetic equation. We thus believe that the Hikami box is described by an equation without such term [i.e., analogous to our Eqs. (39) and (43) in the absence of perturbation,  $\delta \mathcal{U}, \tilde{\tau}_{tr}^{-1} = 0$ ] but with appropriate boundary conditions. While this will probably not affect the main results of Ref. [19] (depending only logarithmically on  $\tau_q$ ), such a more consistent treatment of the quasiclassical Hikami box [31] would be of conceptual importance for the theory of quantum interference effects in systems with large-scale inhomogeneities. We leave this issue as an open problem for the future research.

## ACKNOWLEDGMENTS

Discussions with B. Shapiro are gratefully acknowledged. This work was supported by the SFB195 der Deutschen Forschungsgemeinschaft, by the German-Israeli Foundation, and

by the RFBR. A part of this work was done when two of us (I.V.G. and A.D.M.) participated in the program “Chaos and Interactions: from Nuclei to Quantum Dots” of the Institute for Nuclear Theory at the University of Washington, Seattle. We acknowledge the Institute for Nuclear Theory for hospitality and partial support.

- 
- [1] A. Peres, *Quantum Theory: Concepts and Methods* (Kluwer Academic, Dordrecht, 1993).
- [2] A. Peres, Phys. Rev. A **30**, 1610 (1984).
- [3] R.A. Jalabert and H.M. Pastawski, Phys. Rev. Lett. **86**, 2490 (2001).
- [4] H.M. Pastawski, P.R. Levstein, G. Usaj, J. Raya, and J. Hirschinger, Physica A **283**, 166 (2000).
- [5] F.M. Cucchietti, H.M. Pastawski, and D.A. Wisniacki, Phys. Rev. E **65**, 045206(R) (2002).
- [6] P. Jacquod, P.G. Silvestrov, and C.W.J. Beenakker, Phys. Rev. E **64**, 055203 (2001).
- [7] F.M. Cucchietti, C.H. Lewenkopf, E.R. Mucciolo, H.M. Pastawski, and R.O. Vallejos, Phys. Rev. E **65**, 046209 (2002).
- [8] G. Benenti and G. Casati, Phys. Rev. E **65**, 066205 (2002).
- [9] N.R. Cerruti and S. Tomsovic, Phys. Rev. Lett. **88**, 054103 (2002).
- [10] T. Prosen, Phys. Rev. E **65**, 036208 (2002).
- [11] P.G. Silvestrov and C.W.J. Beenakker, Phys. Rev. E **65**, 035208 (2002).
- [12] P. Silvestrov, J. Tworzydło, and C. Beenakker, Phys. Rev. E **67**, 025204(R) (2003).
- [13] G. Benenti, G. Casati, and G. Veble, e-print nlin.CD/0208003.
- [14] P. Jacquod, I. Adagideli, and C.W.J. Beenakker, Phys. Rev. Lett. **89**, 154103 (2002).
- [15] Z.P. Karkuszewski, C. Jarzynski, and W.H. Zurek, Phys. Rev. Lett. **89**, 170405 (2002).
- [16] D.A. Wisniacki and D. Cohen, Phys. Rev. E **66**, 046209 (2002).
- [17] T. Prosen and M. Znidaric, J. Phys. A **35**, 1455 (2002).
- [18] T. Prosen and T.H. Seligman, J. Phys. A **35**, 4707 (2002).
- [19] I.L. Aleiner and A.I. Larkin, Phys. Rev. B **54**, 14 423 (1996).
- [20] I.L. Aleiner and A.I. Larkin, Phys. Rev. E **55**, R1243 (1997).
- [21] O. Agam, I. Aleiner, and A. Larkin, Phys. Rev. Lett. **85**, 3153 (2000).
- [22] M. Vavilov and A. Larkin, Phys. Rev. B **67**, 115335 (2003).
- [23] I.V. Gornyi and A.D. Mirlin, J. Low Temp. Phys. **126**, 1339 (2002).
- [24] B. Spivak and A. Zyuzin, in *Mesoscopic Phenomena in Solids*, edited by B. Altshuler, P. Lee, and R. Webb (Elsevier Science, North-Holland, Amsterdam, 1991), p. 37.
- [25] B. Shapiro, Phys. Rev. Lett. **57**, 2168 (1986); R. Pnini and B. Shapiro, Phys. Rev. B **39**, 6986 (1989).
- [26] M. Stephen, in *Mesoscopic Phenomena in Solids*, edited by B. Altshuler, P. Lee, and R. Webb (Elsevier Science, North-Holland, Amsterdam, 1991), p. 81.
- [27] B. Altshuler and B. Spivak, Pis'ma Zh. Eksp. Teor. Fiz. **42**, 363 (1985) [JETP Lett. **42**, 447 (1985)].
- [28] P. Wölfle and R.N. Bhatt, Phys. Rev. B **30**, 3542 (1984).
- [29] A.D. Mirlin, E. Altshuler, and P. Wölfle, Ann. Phys. (Leipzig) **5**, 281 (1996).
- [30] In the opposite case  $l_L \ll \tilde{l}_s$  (which is the case if the perturbation is very weak, or if the potential is not sufficiently long ranged), the Lyapunov regime does not exist, and the golden-rule decay crosses over directly to a power-law ballistic-diffuson regime.
- [31] For other recent works in this direction see R.S. Whitney, I.V. Lerner, and R.A. Smith, Waves Random Media **9**, 179 (1999); M. Sieber and K. Richter, Phys. Scr. T **90**, 128 (2001); K. Richter and M. Sieber, Phys. Rev. Lett. **89**, 206801 (2002); V.R. Kogan and K.B. Efetov, e-print cond-mat/0211258.